Retardation and repair of fatigue cracks in a microcapsule toughened epoxy composite—Part II: *In situ* self-healing

E.N. Brown[1,*], S.R. White[2], N.R. Sottos[1]

[1] Department of Theoretical and Applied Mechanics and the Beckman Institute for Advanced Science and Technology, University of Illinois at Urbana-Champaign, Urbana, IL 61801, USA

[2] Department of Aerospace Engineering and the Beckman Institute for Advanced Science and Technology, University of Illinois at Urbana-Champaign, Urbana, IL 61801, USA

[*] Corresponding Author. Present address: Materials Science and Technology Division, Los Alamos National Laboratory, MS-E544, Los Alamos, NM 87545, USA. Tel: 1(505)667-0799, Fax: 1(505)667-2185.

E-mail address: en_brown@lanl.gov (E.N. Brown).

Abstract

Successful arrest and retardation of fatigue cracks is achieved with an *in situ* self-healing epoxy matrix composite that incorporates microencapsulated dicyclopentadiene (DCPD) healing agent and Grubbs' first generation Ru catalyst. Healing agent is released into the crack plane by the propagating crack, where it polymerizes to form a polymer wedge, generating a crack tip shielding mechanism. Due to the complex kinetics of healing a growing crack, the resulting *in situ* retardation and arrest of fatigue cracks exhibit a strong dependence on the applied range of cyclic stress intensity ΔK_I. Significant crack arrest and life extension result when the *in situ* healing rate is faster than the crack growth rate. In loading cases where the crack grows too rapidly (maximum applied stress intensity factor is a significant percentage of the mode-I fracture toughness value), a carefully timed rest period can be used to prolong fatigue life up to 118%. At moderate ΔK_I, *in situ* healing extends fatigue life by as much as 213%. Further improvements in fatigue life-extension are achieved by employing a rest period, which leads to permanent arrest at this moderate ΔK_I. At lower values of applied stress intensity factor, self-healing yields complete arrest of fatigue cracks providing infinite fatigue life-extension.

Keywords: A. smart materials, A. polymer-matrix composites, B. fatigue, D. fractography, self-healing

---

Submitted for publication in *Composites Science and Technology* (2005)

1. Introduction

Self-healing materials are inspired by living systems in which damage triggers an autonomic healing response. White et al. [1] have developed a self-healing polymer that mimics many of the features of a biological system. Healing is accomplished by incorporating a microencapsulated healing agent and a catalytic chemical trigger within a polymer matrix. Damage in the form of a crack initiates the self-healing process, as does the fracture event in biological systems. The approaching crack ruptures the embedded microcapsules, releasing healing agent into the crack plane through capillary action. Polymerization of the healing agent is activated by contact with the embedded catalyst, bonding the crack faces.

Successful self-healing has been demonstrated for an epoxy composite modified with 5-25 wt% microencapsulated dicyclopentadiene (DCPD) monomer and 2.5 wt% Grubbs' first generation transition metal (Ru) catalyst. The embedded microcapsules were shown to rupture in the presence of a crack and release the DCPD monomer into the crack plane. Contact with the embedded Grubbs' catalyst [2] initiated ring opening metathesis polymerization (ROMP) of the DCPD [3,4] and rebonded the crack plane. This self-healing epoxy was able to recover over 90% of its virgin fracture toughness [5] and provide recovery from delamination damage in a reinforced composite [6,7]. In addition to providing an efficient mechanism for self-healing, the presence of DCPD-filled polymeric microcapsules also increased the inherent fracture toughness of the epoxy. Under monotonic loading the maximum toughness with microcapsules was 127% greater than neat epoxy [8]. The increased toughening associated with fluid-filled microcapsules was attributed to crack pinning along with increased hackle marking and subsurface microcracking. Brown et al. [9] also investigated the influence of microcapsules on fatigue crack propagation behavior of epoxy with the effects of self-healing precluded. The addition of microcapsules significantly decreased the fatigue crack growth rate and increased the fatigue life above a transition value of the stress intensity factor [9].

In the current work, we investigate the performance of this successful self-healing epoxy system under cyclic loading (fatigue) conditions. Characterization of fatigue response is more complex than monotonic fracture due to dependence on the applied stress intensity range $\Delta K_I = K_{max}-K_{min}$, the loading frequency f, the ratio of applied stress intensity $R=K_{max}/K_{min}$, as well as the healing kinetics and any rest periods employed. Only a few studies of fatigue crack healing have been reported in the literature for polymeric materials. Daniel and Kim [10] investigated fatigue damage in asphalt by measuring the increase in the specimen compliance as microcrack growth occurred. After a rest period, gains in stiffness were observed and attributed to healing of the microcracks. Zako and Takano [11] performed a tensile fatigue test on a notched specimen to investigate crack healing in an epoxy composite. The specimen was fatigued until the stiffness decreased by 12.5%. The test was stopped and the crack was healed by application of heat, which triggered flow and subsequent polymerization of embedded particles of B-staged resin. The fatigue test was resumed with almost full recovery of stiffness. Following healing, the stiffness decreased at a similar rate to the virgin specimen. Both of these investigations considered successful healing as the recovery of stiffness lost due to damage induced by cyclic loading. Neither the effect on crack-growth rate or absolute fatigue life was considered.

In Part I of this paper [12], we reported successful healing of fatigue cracks through manual injection of precatalyzed DCPD resin into the crack plane. Healing efficiency was defined by the fatigue life-extension,

$$\lambda = \frac{N_{\text{healed}} - N_{\text{control}}}{N_{\text{control}}}, \tag{1}$$

where N_{healed} is the total number of cycles to failure for the self-healing sample and N_{control} is the total number of cycles to failure for a similar sample without healing. Just after injection, the viscous polymer in the crack effectively shielded the crack tip and slowed crack growth. With time, a polyDCPD wedge was formed at the crack tip, leading to artificial crack closure and fatigue life-extension of $\lambda > 2000\%$. In Part II, we build on the success of these mechanisms for retarding fatigue crack growth to achieve the first demonstration of *in situ* self-healing of fatigue damage.

2. Fatigue test method

2.1. Materials and specimen preparation

Materials, specimen preparation and testing were nearly identical to that described in Part I of this paper [12]. Tapered double-cantilever beam specimens were cast from EPON® 828 epoxy resin (DGEBA) and 12 pph Ancamine® DETA (diethylenetriamine) curing agent with 20 wt% 180 μm diameter microcapsules [13] and 2.5 wt% Grubbs' catalyst mixed into the resin. The microcapsule concentration of 20 wt% was chosen to ensure adequate presence of healing agent in the crack plane. Control samples were also fabricated with no catalyst (only microcapsules) to preclude the effects of self-healing. The epoxy mixtures were degassed, poured into a closed silicone rubber mold and cured for 24 hours at room temperature, followed by 24 hours at 30° C.

2.2. Mechanical testing

The fatigue-crack propagation behavior of the self-healing epoxy was investigated using the tapered double-cantilever beam (TDCB) specimen geometry presented in Part I of this paper [12]. The TDCB geometry provides a crack length independent relationship between the applied stress intensity factor ΔK_{I} and load ΔP,

$$K_{\text{I}} = \alpha P, \tag{2}$$

where $\alpha = 11.2\text{x}10^{3}\ \text{m}^{-3/2}$ for the current system [5]. Samples were precracked and immediately cyclically loaded. A triangular frequency of 5 Hz was applied with a load ratio ($R = K_{\min}/K_{\max}$) of 0.1. Crack lengths were measured optically and by a calibration based on specimen compliance [9,12]. Each loading condition was investigated with continuous cyclic loading to sample failure and with rest periods to allow for healing with stationary crack faces. In all cases, fatigue crack growth in a self-healing sample was compared to that in a control sample (with no healing) under identical loading conditions and healing efficiency evaluated via Eq. (1).

3. Self-healing of the *in situ* system

In situ healing was investigated by measuring the fatigue life-extension of samples manufactured with 20 wt% microcapsules and 2.5 wt% catalyst. For successful *in situ* self-healing, the healing agent released into the crack plane must have enough time to polymerize. If the crack growth rate is too fast, little or no healing will occur. In previous work, Brown et al. [5] measured the development of healing efficiency in this same materials system through monotonic fracture tests performed at prescribed times following the initial virgin fracture. After an initial dwell period of about 25 min during which no appreciable healing was measured, the healing efficiency increased exponentially and stabilized at maximum healing efficiency after about 10 h (see Fig. 1). Comparison of the development of healing efficiency with the degree of cure (α) for bulk DCPD measured by Kessler and White [3] using differential scanning calorimetry (DSC) shows a similar exponential relationship with time (Fig. 1). Moreover, the development of measurable healing efficiency at 25 min closely corresponds to α=1/3, the theoretical gel point for a tetrafunctional monomer such as polyDCPD [14].

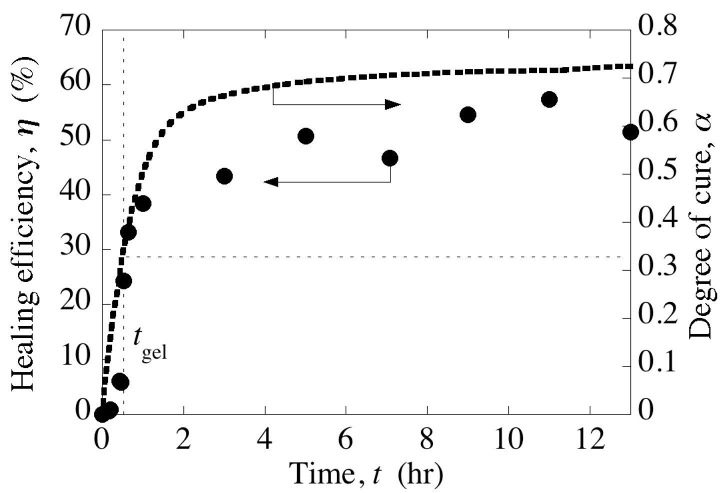

Fig. 1. Comparison between the development of healing efficiency and degree of cure of DCPD. Healing efficiency was obtained from monotonic fracture tests performed at prescribed times following the initial virgin fracture [5]. Differential scanning calorimetry (DSC) was used to measure degree of cure data for 30°C isothermal polymerization of DCPD with 2 g L^{-1} of Grubbs' catalyst [3].

Anticipating that the competition between polymerization kinetics and mechanical crack growth would be a major factor influencing successful healing, three different levels of applied range of stress intensity ΔK_I were prescribed, one low-cycle fatigue case and two high-cycle fatigue cases. Low-cycle fatigue refers to the fatigue regime where ΔK_I approaches K_{IC} and rapid crack growth causes sample failure after very few cycles

(< 10,000 cycles). High-cycle fatigue refers to the fatigue regime of low ΔK_I, relatively slow crack growth rate and longer fatigue life (> 10,000 cycles).

3.1. In situ low-cycle (high ΔK_I) fatigue-healing

Under low-cycle fatigue conditions ($N_{healed} < 10{,}000$), crack propagation in the self-healing epoxy proceeded at a constant rate (Fig. 2) comparable to a control sample with no self-healing. Control sample data were virtually identical to the self-healing sample data indicating no retardation was taking place due to healing because crack propagation was so rapid. Sample fatigue life in the low-cycle fatigue regime was much shorter (2.5 x 10^4 cycles ~1.4 h) than the 10 hours necessary for the healing agent to fully polymerize in the crack plane. The fatigue life-extension was essentially zero, $\lambda \sim 0\%$. The effect of rest periods was also investigated on two additional low-cycle fatigue cases. In the first case, loading was stopped after a small amount of crack growth and the samples were allowed to heal unloaded for 10 h to ensure full cure of the healing agent. The crack tip regressed to the approximate position of the TDCB notch, as shown in Fig. 3. However, after only a few cycles the crack tip rapidly progressed through the healed region to its location prior to healing. The fatigue healing efficiency λ for this case was essentially zero.

In the second case, fatigue loading was stopped after a small amount of crack growth and healing was allowed under load at K_{max} for 10 h. Figure 2 shows the regression and retardation of a fatigue crack achieved in this case. Similar to the samples repaired by manual injection described in Part I of this paper [12], healing while loaded at K_{max} was much more effective. Under these conditions, polymerized healing agent formed a wedge at the crack tip, as shown in profile by optical microscopy in Fig. 4a. Electron micrographs of the fracture plane (Fig. 4b,c), revealed that the polymer wedge

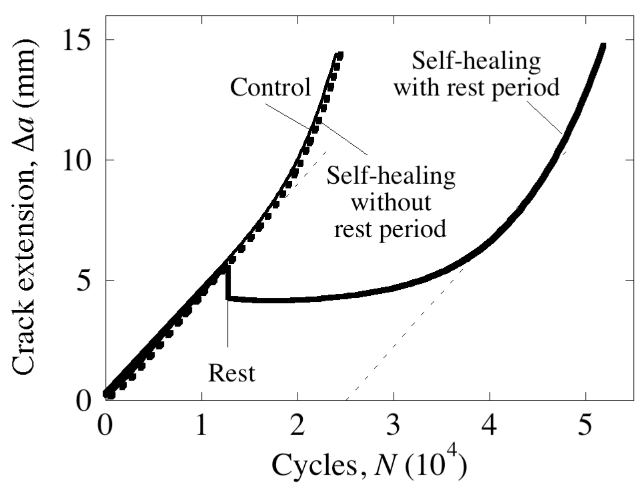

Fig. 2. Crack length *vs.* fatigue cycles of *in situ* sample tested in low-cycle fatigue regime without and with a rest period (under load at K_{max}), $\lambda = 0$ and 118% respectively. $\Delta K_I = 0.405$ MPa m$^{1/2}$, $K_{max} = 0.450$ MPa m$^{1/2}$, $K_{min} = 0.045$ MPa m$^{1/2}$, $R = 0.1$, $f = 5$ Hz, and $a_0 = 31.2$ mm.

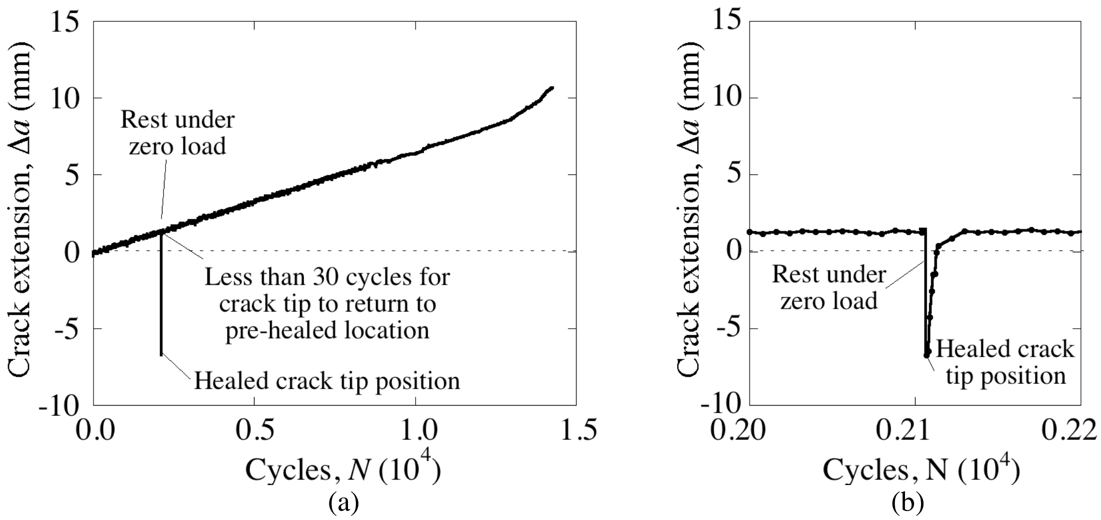

Fig. 3. Crack length *vs*. fatigue cycles of *in situ* sample with a rest period in the unloaded configuration, $\lambda \cong 0.2\%$. (a) Plotted for the entire fatigue life and (b) plotted in the region of the rest period. $\Delta K_I = 0.472$ MPa m$^{1/2}$ $K_{max} = 0.524$ MPa m$^{1/2}$, $K_{min} = 0.052$ MPa m$^{1/2}$, $R = 0.1$, $f = 5$ Hz, and $a_0 = 30.2$ mm.

consisted of a region of polyDCPD extending ~1 mm from the crack tip. The wedge penetrated into the sharp tip of the crack along the majority of the crack front line and had a significant out-of-plane thickness away from the crack tip. Because the interface was formed at K_{max}, it was under zero stress when the applied cyclic load reached K_{max} and under a compressive stress at all other points in the cycle. Under low-cycle-fatigue conditions ($N_{healed} < 10{,}000$, high ΔK_I) fatigue life-extension λ for *in situ* self-healing epoxy with a rest period at K_{max} ranged from 73–118% for three samples. The 1–2 mm regression of the crack tip due to self-healing calculated from compliance measurements corresponded with direct microscopy measurements of the polymer wedge at the crack tip.

3.2. In situ high-cycle (low ΔK_I) fatigue-healing

Under high-cycle fatigue conditions ($N_{healed} > 10{,}000$) the applied range of stress intensity ΔK_I was reduced, decreasing the crack growth rate and increasing the number of cycles to sample failure. In this regime, the sample fatigue life exceeded the time for the healing agent to gel (and quasistatic healing efficiency to develop). Self-healing fatigue life-extension was investigated for a number of samples under this type of loading. The effect of rest periods was also considered.

In situ samples were precracked and fatigued to failure. A typical plot of crack length *vs*. fatigue cycles is shown in Fig. 5. The initial release of healing agent during precracking retarded the crack growth, and led to some crack regression. Following this period of crack arrest, the crack eventually grew past the healed precrack (~ 3.5×10^5 cycles). After this point, the fatigue crack growth behavior transitioned between periods of constant crack growth rate and periods of crack retardation. During

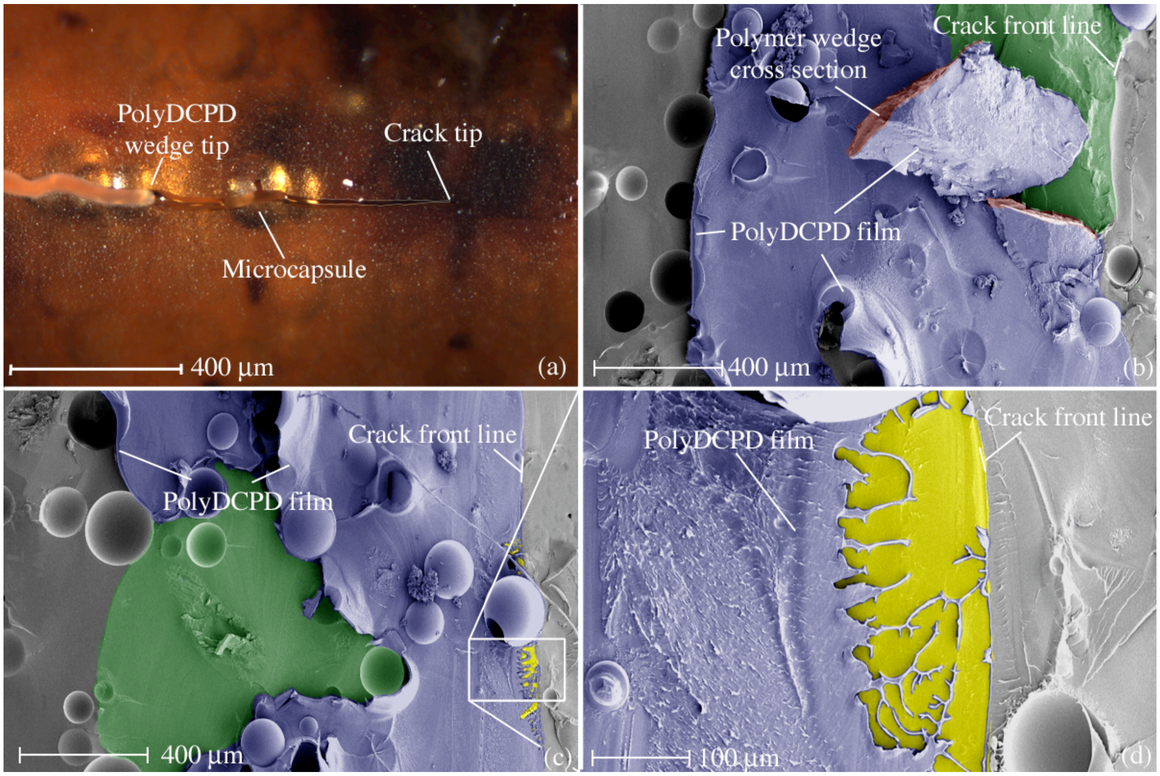

Fig. 4. PolyDCPD wedge at the crack tip of *in situ* sample tested in low-cycle fatigue regime with a rest period under load (see Fig. 2). (a) Optical micrograph of crack tip side view following rest period. The polymer wedge extends ~1 mm from the crack tip. (b) SEM micrograph of the fracture surface in the region of the crack tip. The polyDCPD wedge (blue) extends ~1 mm from the crack tip, with the cross section (red) tapering from a finite thickness to a sharp point at the crack tip. The region of the fracture surface where the polyDCPD has separated from the epoxy matrix is indicated in green. (c,d) PolyDCPD fills the crack to the tip along most of the crack front. In some regions, indicated in yellow, the DCPD does not penetrate fully to the crack tip. Note: The crack propagation is from left to right in all images.

the periods of crack retardation, the crack-tip position corresponded to locations of exposed catalyst on the fracture plane. Polymerized healing agent was only present in the vicinity of exposed catalyst and formed an undulating structure with significant out-of-plane dimension, as evidenced by the fracture surface in Fig. 6. The local variation in concentration and imperfect dispersion of catalyst resulted in the localized periods of arrest. Total fatigue life-extension of six samples ranged from 89–213% and was amplified by increasing both the number of arrest events (*i.e.* increasing the number of catalyst particles exposed) and the duration of the individual arrest events. The recent development of wax-protected catalyst for self-healing by Rule *et al.* [15]—yielding improved dispersion of catalyst with increased reactivity—has the potential to provide more uniform an effective *in situ* healing in this loading regime, ultimately yielding even greater fatigue life-extension.

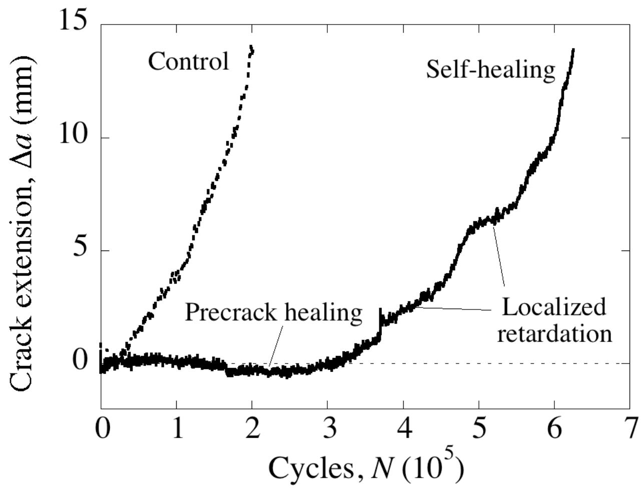

Fig. 5. Crack length *vs*. fatigue cycles of *in situ* sample tested to failure in high-cycle fatigue regime, $\lambda = 213\%$. $\Delta K_I = 0.338$ MPa m$^{1/2}$, $K_{max} = 0.376$ MPa m$^{1/2}$, $K_{min} = 0.038$ MPa m$^{1/2}$, $R = 0.1$, $f = 5$ Hz, and $a_0 = 35.4$ mm.

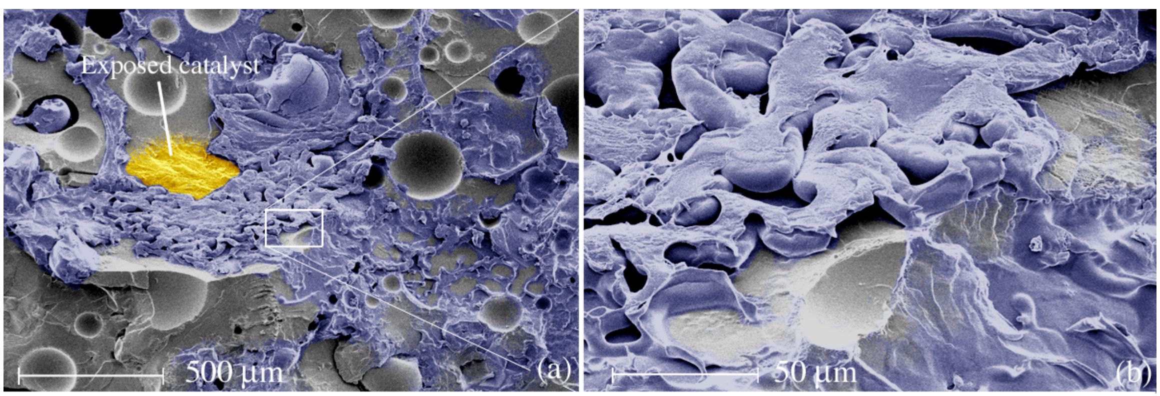

Fig. 6. (a) SEM micrograph of the *in situ* healed polyDCPD film (blue) on fatigue surface in the vicinity of a sites of exposed catalyst (orange). (b) The film forms an undulating structure due to cyclic loading during cure. Note: The crack propagation is from left to right in both images.

The fatigue life-extension due to precrack healing was dramatically improved by adding a rest period at K_{max}. *In situ* samples healed for 10 h at K_{max} following precracking and tested in the high-cycle fatigue regime exhibited permanent crack arrest in the two samples tested (see Fig. 7). As in the low-cycle fatigue case healed at K_{max}, a solid polyDCPD wedge formed at the crack tip during the rest period, with similar effect. The retardation elicited by the wedge was more efficient in this regime of loading. If K_{max} was reduced even further ($\Delta K_I < 0.5\ K_{IC}$), threshold conditions were achieved without a rest period. As shown in Fig. 8, the precrack regressed approximately 1 mm and never progressed further in the time frame of the test. In contrast, the precrack in the control sample was slowly growing at a constant rate. This effect was observed repeatably in four samples tested. Again, the healing agent released during the precrack event formed a partial polymer wedge at the crack tip (Fig. 9). Similar to the polyDCPD formed in the cycling crack under higher K_{max} (Fig. 6), the wedge created under lower cyclic load conditions had undulating surface features, but covered far more of the crack plane. A summary of life extension values under the different loading conditions is given in Table 1.

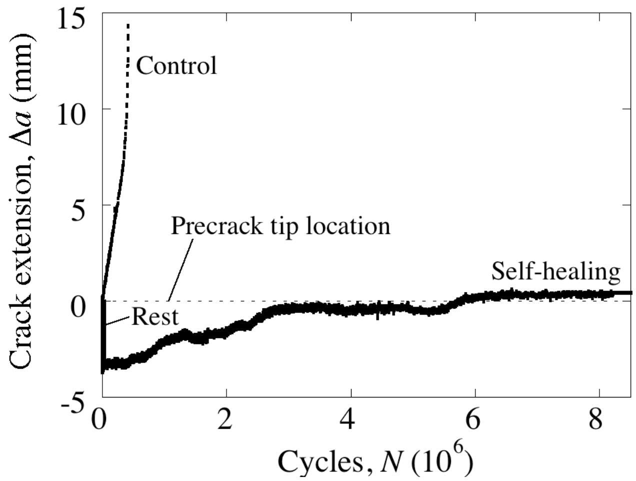

Fig. 7. Crack length *vs*. fatigue cycles of *in situ* sample tested in high-cycle fatigue regime with a rest period of 10 h at K_{max} after precracking, $\lambda = \infty$. $\Delta K_I = 0.338$ MPa m$^{1/2}$, $K_{max} = 0.376$ MPa m$^{1/2}$, $K_{min} = 0.038$ MPa m$^{1/2}$, $R = 0.1$, $f = 5$ Hz, and $a_0 = 31.6$ mm.

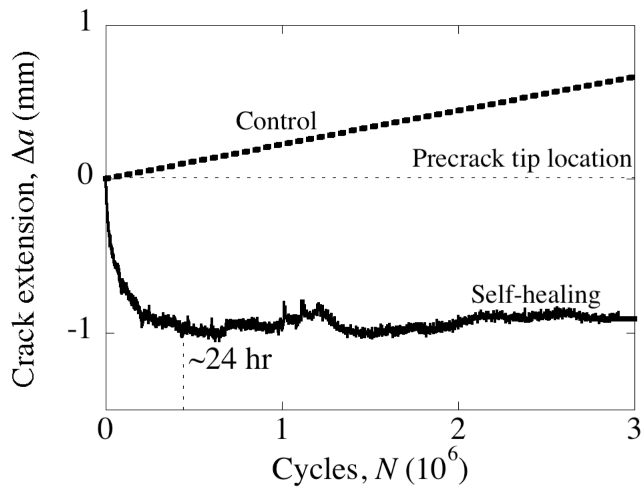

Fig. 8. Crack length *vs*. fatigue cycles of *in situ* sample in the threshold regime, $\lambda = \infty$. $\Delta K_I = 0.270$ MPa m$^{1/2}$, $K_{max} = 0.300$ MPam$^{1/2}$, $K_{min} = 0.030$ MPa m$^{1/2}$, $R = 0.1$, $f = 5$ Hz, and $a_0 = 29.7$ mm.

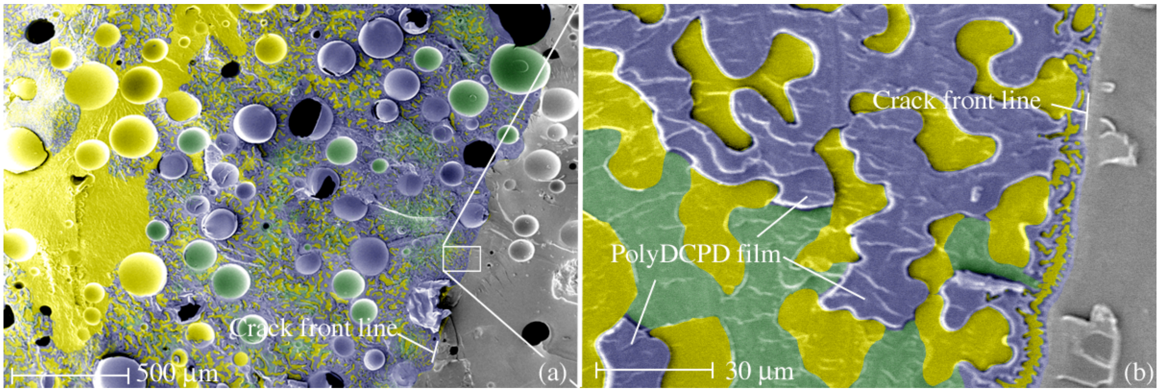

Fig. 9. SEM micrograph of the polyDCPD wedge at the crack tip of *in situ* sample tested in high-cycle fatigue regime resulting in crack arrest. (a) Image of the fracture surface in the region of the crack tip. The polyDCPD wedge (blue) extends from the crack tip forming a wavy pattern with many areas uncovered by polyDCPD (yellow). The region of the fracture surface where the polyDCPD has separated from the epoxy matrix is indicated in green. (b) PolyDCPD fills the crack to the tip along most of the crack front. Note: The crack propagation is from left to right in both images.

Table 1
Fatigue life-extension from self-healing

Regime	Range of applied stress intensity, ΔK_I (MPa m$^{1/2}$)	Fatigue life-extension, λ	
		Continuously cycled to failure	With one rest period at K_{max}
$t_{fail} << t_{heal}$	0.7–0.9 K_{IC}	~0%	73–118%
$t_{fail} \sim t_{heal}$	0.5–0.7 K_{IC}	89–213%	∞^a
$t_{fail} >> t_{heal}$	< 0.5 K_{IC}	∞	—

[a] Infinite fatigue life-extension denotes no optically measurable crack extension after at least 3×10^6 cycles (7 days of testing). Note: $t_{heal} \sim 10$ h from monotonic fracture [5].

4. Conclusions

The crack growth behavior of self-healing epoxy under fatigue loading was investigated using a protocol based on fatigue life-extension. Significant crack arrest and life extension resulted when the *in situ* healing rate was faster than the crack growth rate. In loading cases where the crack grew too rapidly (maximum applied stress intensity factor is a significant percentage of the mode-I fracture toughness value), carefully timed rest periods were used to prolong fatigue life. At lower values of applied stress intensity factor, crack growth was arrested completely. The self-healing material system demonstrated great potential for extending component life under fatigue loading, with the degree of life extension dependent on a number of interrelated variables such as stress amplitude, frequency, *in situ* healing rate, and rest periods.

Fatigue life-extension from *in situ* self-healing was achieved by a combination of crack-tip shielding mechanisms. First, viscous flow of the healing agent in the crack plane retarded crack growth. Second, polymerization of the healing agent provided a short term adhesive effect and a long term crack closure effect, which prevented unloading of the crack tip. Successful healing resulted in reduced crack length and retardation of additional crack growth. These shielding mechanisms also contributed to increasing the threshold ΔK_{th}, effectively increasing the amplitude of applied ΔK_I that the material can be subjected to without crack propagation. Above the threshold ΔK_{th}, the self-healing shielding mechanisms led to temporary arrest of fatigue crack growth and significantly extended fatigue life.

The dominant shielding mechanism observed for *in situ* self-healing was crack closure induced by the formation of a polyDCPD wedge at the crack tip. Similar to the case of artificial crack closure achieved by manual injection, the profile of the load–displacement curves progresses from linear to bi-modal as the crack propagates through the healed region.

The success of crack closure was strongly dependent on how efficiently the crack tip was shielded from the applied cyclic loads. A polymer wedge formed at or above K_{max} provided maximum shielding, approaching a stress free crack tip. Conversely a polymer wedge polymerized at zero-load provided minimal crack tip shielding. Because the polymer wedge formed under continuous cyclic loading was created between moving boundaries, the wedge structure was irregular and resulted in shielding efficiency between the two extremes.

Acknowledgments

The authors gratefully acknowledge support from the AFOSR Aerospace and Materials Science Directorate Mechanics and Materials Program (Award No. F49620-02-1-0080), the National Science Foundation (NSF CMS0218863), and Motorola Labs, Motorola Advanced Technology Center, Schaumburg Ill. The authors would also like to thank Profs. J.S. Moore and P.H. Geubelle of the University of Illinois at Urbana-Champaign and Dr. A. Skipor of Motorola Labs for technical support and helpful discussions. Electron microscopy was performed in the Imaging Technology Group, Beckman Institute, of the University of Illinois at Urbana-Champaign, with the assistance of S. Robinson.

References

[1] White SR, Sottos NR, Geubelle PH, Moore JS, Kessler MR, Sriram SR, Brown EN, Viswanathan S. Autonomic healing of polymer composites. Nature 2001;409(6822): 794–797.

[2] Dias EL, Nguyen ST, Grubbs RH. Well-defined ruthenium olefin metathesis catalysts: Mechanism and activity. J Am Chem Soc 1997;119(17):3887–3897.

[3] Kessler MR, White SR. Cure kinetics of the ring-opening metathesis polymerization of dicyclopentadiene. J Polym Sci A 2002;40(14):2373–2383.

[4] Rule JD, Moore JS. ROMP Reactivity of endo- and exo-Dicyclopentadiene. Macromolecules 2002;35(21):7878–7882.

[5] Brown EN, Sottos NR, White SR. Fracture testing of a self-healing polymer composite. Exp Mech 2002;42(4):372–379.

[6] Kessler MR, White SR. Self-activated healing of delamination damage in woven composites. Composites A 2001;32(5):683–699.
[7] Kessler MR, Sottos NR, White SR. Self-healing structural composite materials. Composites A 2003;34(8):743–753.
[8] Brown EN, White SR, Sottos NR. Microcapsule induced toughening in a self-healing polymer composite. J Mater Sci 2004;39(5):1703–1710.
[9] Brown EN, White SR, Sottos NR. Fatigue crack propagation in microcapsule toughened epoxy. J Mater Sci 2004; in review.
[10] Daniel JS, Kim YR. Laboratory evaluation of fatigue damage and healing of asphalt mixtures. J Mater Civil Engng 2001;13(6):434–440.
[11] Zako M, Takano N. Intelligent material systems using epoxy particles to repair microcracks and delamination damage in GFRP. J Intelligent Mater Syst Struct 1999;10(10):836–841.
[12] Brown EN, White SR, Sottos NR. Retardation and repair of fatigue cracks in amicrocapsule toughened epoxy composite—Part I: Manual infiltration. Comp Sci Tech 2004; submitted.
[13] Brown EN, Kessler MR, Sottos NR, White SR. In situ poly(urea-formaldehyde) microencapsulation of dicyclopentadiene. J Microencap 2003;20(16):719–730.
[14] Miller DR, Macosko CW. A new derivation of post gel properties of network polymers. Macromolecules 1976;9(2):206–211.
[15] Rule JD, Brown EN, Sottos NR, White SR, Moore JS. Wax-protected catalyst microspheres for efficient self-healing materials. Adv Mater 2005;17(2)205–208.

List of Recent TAM Reports

No.	*Authors*	*Title*	*Date*
978	Sofronis, P., I. M. Robertson, Y. Liang, D. F. Teter, and N. Aravas	Recent advances in the study of hydrogen embrittlement at the University of Illinois—Invited paper, Hydrogen–Corrosion Deformation Interactions (Sept. 16–21, 2001, Jackson Lake Lodge, Wyo.)	Sept. 2001
979	Fried, E., M. E. Gurtin, and K. Hutter	A void-based description of compaction and segregation in flowing granular materials—*Continuum Mechanics and Thermodynamics*, in press (2003)	Sept. 2001
980	Adrian, R. J., S. Balachandar, and Z.-C. Liu	Spanwise growth of vortex structure in wall turbulence—*Korean Society of Mechanical Engineers International Journal* **15**, 1741–1749 (2001)	Sept. 2001
981	Adrian, R. J.	Information and the study of turbulence and complex flow—*Japanese Society of Mechanical Engineers Journal B*, in press (2002)	Oct. 2001
982	Adrian, R. J., and Z.-C. Liu	Observation of vortex packets in direct numerical simulation of fully turbulent channel flow—*Journal of Visualization*, in press (2002)	Oct. 2001
983	Fried, E., and R. E. Todres	Disclinated states in nematic elastomers—*Journal of the Mechanics and Physics of Solids* **50**, 2691–2716 (2002)	Oct. 2001
984	Stewart, D. S.	Towards the miniaturization of explosive technology—Proceedings of the 23rd International Conference on Shock Waves (2001)	Oct. 2001
985	Kasimov, A. R., and Stewart, D. S.	Spinning instability of gaseous detonations—*Journal of Fluid Mechanics* (submitted)	Oct. 2001
986	Brown, E. N., N. R. Sottos, and S. R. White	Fracture testing of a self-healing polymer composite—*Experimental Mechanics* (submitted)	Nov. 2001
987	Phillips, W. R. C.	Langmuir circulations—*Surface Waves* (J. C. R. Hunt and S. Sajjadi, eds.), in press (2002)	Nov. 2001
988	Gioia, G., and F. A. Bombardelli	Scaling and similarity in rough channel flows—*Physical Review Letters* **88**, 014501 (2002)	Nov. 2001
989	Riahi, D. N.	On stationary and oscillatory modes of flow instabilities in a rotating porous layer during alloy solidification—*Journal of Porous Media* **6**, 1–11 (2003)	Nov. 2001
990	Okhuysen, B. S., and D. N. Riahi	Effect of Coriolis force on instabilities of liquid and mushy regions during alloy solidification—*Physics of Fluids* (submitted)	Dec. 2001
991	Christensen, K. T., and R. J. Adrian	Measurement of instantaneous Eulerian acceleration fields by particle-image accelerometry: Method and accuracy—*Experimental Fluids* (submitted)	Dec. 2001
992	Liu, M., and K. J. Hsia	Interfacial cracks between piezoelectric and elastic materials under in-plane electric loading—*Journal of the Mechanics and Physics of Solids* **51**, 921–944 (2003)	Dec. 2001
993	Panat, R. P., S. Zhang, and K. J. Hsia	Bond coat surface rumpling in thermal barrier coatings—*Acta Materialia* **51**, 239–249 (2003)	Jan. 2002
994	Aref, H.	A transformation of the point vortex equations—*Physics of Fluids* **14**, 2395–2401 (2002)	Jan. 2002
995	Saif, M. T. A, S. Zhang, A. Haque, and K. J. Hsia	Effect of native Al_2O_3 on the elastic response of nanoscale aluminum films—*Acta Materialia* **50**, 2779–2786 (2002)	Jan. 2002
996	Fried, E., and M. E. Gurtin	A nonequilibrium theory of epitaxial growth that accounts for surface stress and surface diffusion—*Journal of the Mechanics and Physics of Solids* **51**, 487–517 (2003)	Jan. 2002
997	Aref, H.	The development of chaotic advection—*Physics of Fluids* **14**, 1315–1325 (2002); see also *Virtual Journal of Nanoscale Science and Technology*, 11 March 2002	Jan. 2002
998	Christensen, K. T., and R. J. Adrian	The velocity and acceleration signatures of small-scale vortices in turbulent channel flow—*Journal of Turbulence*, in press (2002)	Jan. 2002
999	Riahi, D. N.	Flow instabilities in a horizontal dendrite layer rotating about an inclined axis—*Journal of Porous Media*, in press (2003)	Feb. 2002

List of Recent TAM Reports (cont'd)

No.	Authors	Title	Date
1000	Kessler, M. R., and S. R. White	Cure kinetics of ring-opening metathesis polymerization of dicyclopentadiene—*Journal of Polymer Science A* **40**, 2373–2383 (2002)	Feb. 2002
1001	Dolbow, J. E., E. Fried, and A. Q. Shen	Point defects in nematic gels: The case for hedgehogs—*Archive for Rational Mechanics and Analysis*, in press (2004)	Feb. 2002
1002	Riahi, D. N.	Nonlinear steady convection in rotating mushy layers—*Journal of Fluid Mechanics* **485**, 279–306 (2003)	Mar. 2002
1003	Carlson, D. E., E. Fried, and S. Sellers	The totality of soft-states in a neo-classical nematic elastomer—*Journal of Elasticity* **69**, 169–180 (2003) with revised title	Mar. 2002
1004	Fried, E., and R. E. Todres	Normal-stress differences and the detection of disclinations in nematic elastomers—*Journal of Polymer Science B: Polymer Physics* **40**, 2098–2106 (2002)	June 2002
1005	Fried, E., and B. C. Roy	Gravity-induced segregation of cohesionless granular mixtures—*Lecture Notes in Mechanics*, in press (2002)	July 2002
1006	Tomkins, C. D., and R. J. Adrian	Spanwise structure and scale growth in turbulent boundary layers—*Journal of Fluid Mechanics* (submitted)	Aug. 2002
1007	Riahi, D. N.	On nonlinear convection in mushy layers: Part 2. Mixed oscillatory and stationary modes of convection—*Journal of Fluid Mechanics* **517**, 71–102 (2004)	Sept. 2002
1008	Aref, H., P. K. Newton, M. A. Stremler, T. Tokieda, and D. L. Vainchtein	Vortex crystals—*Advances in Applied Mathematics* **39**, in press (2002)	Oct. 2002
1009	Bagchi, P., and S. Balachandar	Effect of turbulence on the drag and lift of a particle—*Physics of Fluids*, in press (2003)	Oct. 2002
1010	Zhang, S., R. Panat, and K. J. Hsia	Influence of surface morphology on the adhesive strength of aluminum/epoxy interfaces—*Journal of Adhesion Science and Technology* **17**, 1685–1711 (2003)	Oct. 2002
1011	Carlson, D. E., E. Fried, and D. A. Tortorelli	On internal constraints in continuum mechanics—*Journal of Elasticity* **70**, 101–109 (2003)	Oct. 2002
1012	Boyland, P. L., M. A. Stremler, and H. Aref	Topological fluid mechanics of point vortex motions—*Physica D* **175**, 69–95 (2002)	Oct. 2002
1013	Bhattacharjee, P., and D. N. Riahi	Computational studies of the effect of rotation on convection during protein crystallization—*International Journal of Mathematical Sciences*, in press (2004)	Feb. 2003
1014	Brown, E. N., M. R. Kessler, N. R. Sottos, and S. R. White	*In situ* poly(urea-formaldehyde) microencapsulation of dicyclopentadiene—*Journal of Microencapsulation* (submitted)	Feb. 2003
1015	Brown, E. N., S. R. White, and N. R. Sottos	Microcapsule induced toughening in a self-healing polymer composite—*Journal of Materials Science* (submitted)	Feb. 2003
1016	Kuznetsov, I. R., and D. S. Stewart	Burning rate of energetic materials with thermal expansion—*Combustion and Flame* (submitted)	Mar. 2003
1017	Dolbow, J., E. Fried, and H. Ji	Chemically induced swelling of hydrogels—*Journal of the Mechanics and Physics of Solids*, in press (2003)	Mar. 2003
1018	Costello, G. A.	Mechanics of wire rope—Mordica Lecture, Interwire 2003, Wire Association International, Atlanta, Georgia, May 12, 2003	Mar. 2003
1019	Wang, J., N. R. Sottos, and R. L. Weaver	Thin film adhesion measurement by laser induced stress waves—*Journal of the Mechanics and Physics of Solids* (submitted)	Apr. 2003
1020	Bhattacharjee, P., and D. N. Riahi	Effect of rotation on surface tension driven flow during protein crystallization—*Microgravity Science and Technology* **14**, 36–44 (2003)	Apr. 2003
1021	Fried, E.	The configurational and standard force balances are not always statements of a single law—*Proceedings of the Royal Society* (submitted)	Apr. 2003

List of Recent TAM Reports (cont'd)

No.	Authors	Title	Date
1022	Panat, R. P., and K. J. Hsia	Experimental investigation of the bond coat rumpling instability under isothermal and cyclic thermal histories in thermal barrier systems—*Proceedings of the Royal Society of London A* **460**, 1957–1979 (2003)	May 2003
1023	Fried, E., and M. E. Gurtin	A unified treatment of evolving interfaces accounting for small deformations and atomic transport: grain-boundaries, phase transitions, epitaxy—*Advances in Applied Mechanics* **40**, 1–177 (2004)	May 2003
1024	Dong, F., D. N. Riahi, and A. T. Hsui	On similarity waves in compacting media—*Horizons in World Physics* **244**, 45–82 (2004)	May 2003
1025	Liu, M., and K. J. Hsia	Locking of electric field induced non-180° domain switching and phase transition in ferroelectric materials upon cyclic electric fatigue—*Applied Physics Letters* **83**, 3978–3980 (2003)	May 2003
1026	Liu, M., K. J. Hsia, and M. Sardela Jr.	In situ X-ray diffraction study of electric field induced domain switching and phase transition in PZT-5H—*Journal of the American Ceramics Society* (submitted)	May 2003
1027	Riahi, D. N.	On flow of binary alloys during crystal growth—*Recent Research Development in Crystal Growth*, in press (2003)	May 2003
1028	Riahi, D. N.	On fluid dynamics during crystallization—*Recent Research Development in Fluid Dynamics*, in press (2003)	July 2003
1029	Fried, E., V. Korchagin, and R. E. Todres	Biaxial disclinated states in nematic elastomers—*Journal of Chemical Physics* **119**, 13170–13179 (2003)	July 2003
1030	Sharp, K. V., and R. J. Adrian	Transition from laminar to turbulent flow in liquid filled microtubes—*Physics of Fluids* (submitted)	July 2003
1031	Yoon, H. S., D. F. Hill, S. Balachandar, R. J. Adrian, and M. Y. Ha	Reynolds number scaling of flow in a Rushton turbine stirred tank: Part I—Mean flow, circular jet and tip vortex scaling—*Chemical Engineering Science* (submitted)	Aug. 2003
1032	Raju, R., S. Balachandar, D. F. Hill, and R. J. Adrian	Reynolds number scaling of flow in a Rushton turbine stirred tank: Part II—Eigen-decomposition of fluctuation—*Chemical Engineering Science* (submitted)	Aug. 2003
1033	Hill, K. M., G. Gioia, and V. V. Tota	Structure and kinematics in dense free-surface granular flow—*Physical Review Letters*, in press (2003)	Aug. 2003
1034	Fried, E., and S. Sellers	Free-energy density functions for nematic elastomers—*Journal of the Mechanics and Physics of Solids* **52**, 1671–1689 (2004)	Sept. 2003
1035	Kasimov, A. R., and D. S. Stewart	On the dynamics of self-sustained one-dimensional detonations: A numerical study in the shock-attached frame—*Physics of Fluids* (submitted)	Nov. 2003
1036	Fried, E., and B. C. Roy	Disclinations in a homogeneously deformed nematic elastomer—*Nature Materials* (submitted)	Nov. 2003
1037	Fried, E., and M. E. Gurtin	The unifying nature of the configurational force balance—*Mechanics of Material Forces* (P. Steinmann and G. A. Maugin, eds.), in press (2003)	Dec. 2003
1038	Panat, R., K. J. Hsia, and J. W. Oldham	Rumpling instability in thermal barrier systems under isothermal conditions in vacuum—*Philosophical Magazine*, in press (2004)	Dec. 2003
1039	Cermelli, P., E. Fried, and M. E. Gurtin	Sharp-interface nematic–isotropic phase transitions without flow—*Archive for Rational Mechanics and Analysis* **174**, 151–178 (2004)	Dec. 2003
1040	Yoo, S., and D. S. Stewart	A hybrid level-set method in two and three dimensions for modeling detonation and combustion problems in complex geometries—*Combustion Theory and Modeling* (submitted)	Feb. 2004
1041	Dienberg, C. E., S. E. Ott-Monsivais, J. L. Ranchero, A. A. Rzeszutko, and C. L. Winter	Proceedings of the Fifth Annual Research Conference in Mechanics (April 2003), TAM Department, UIUC (E. N. Brown, ed.)	Feb. 2004

No.	Authors	Title	Date
1042	Kasimov, A. R., and D. S. Stewart	Asymptotic theory of ignition and failure of self-sustained detonations—*Journal of Fluid Mechanics* (submitted)	Feb. 2004
1043	Kasimov, A. R., and D. S. Stewart	Theory of direct initiation of gaseous detonations and comparison with experiment—*Proceedings of the Combustion Institute* (submitted)	Mar. 2004
1044	Panat, R., K. J. Hsia, and D. G. Cahill	Evolution of surface waviness in thin films via volume and surface diffusion—*Journal of Applied Physics* (submitted)	Mar. 2004
1045	Riahi, D. N.	Steady and oscillatory flow in a mushy layer—*Current Topics in Crystal Growth Research*, in press (2004)	Mar. 2004
1046	Riahi, D. N.	Modeling flows in protein crystal growth—*Current Topics in Crystal Growth Research*, in press (2004)	Mar. 2004
1047	Bagchi, P., and S. Balachandar	Response of the wake of an isolated particle to isotropic turbulent cross-flow—*Journal of Fluid Mechanics* (submitted)	Mar. 2004
1048	Brown, E. N., S. R. White, and N. R. Sottos	Fatigue crack propagation in microcapsule toughened epoxy—*Journal of Materials Science* (submitted)	Apr. 2004
1049	Zeng, L., S. Balachandar, and P. Fischer	Wall-induced forces on a rigid sphere at finite Reynolds number—*Journal of Fluid Mechanics* (submitted)	May 2004
1050	Dolbow, J., E. Fried, and H. Ji	A numerical strategy for investigating the kinetic response of stimulus-responsive hydrogels—*Journal of the Mechanics and Physics of Solids* (submitted)	June 2004
1051	Riahi, D. N.	Effect of permeability on steady flow in a dendrite layer—*Journal of Porous Media*, in press (2004)	July 2004
1052	Cermelli, P., E. Fried, and M. E. Gurtin	Transport relations for surface integrals arising in the formulation of balance laws for evolving fluid interfaces—*Journal of Fluid Mechanics* (submitted)	Sept. 2004
1053	Stewart, D. S., and A. R. Kasimov	Theory of detonation with an embedded sonic locus—*SIAM Journal on Applied Mathematics* (submitted)	Oct. 2004
1054	Stewart, D. S., K. C. Tang, S. Yoo, M. Q. Brewster, and I. R. Kuznetsov	Multi-scale modeling of solid rocket motors: Time integration methods from computational aerodynamics applied to stable quasi-steady motor burning—*Proceedings of the 43rd AIAA Aerospace Sciences Meeting and Exhibit* (January 2005), Paper AIAA-2005-0357 (2005)	Oct. 2004
1055	Ji, H., H. Mourad, E. Fried, and J. Dolbow	Kinetics of thermally induced swelling of hydrogels—*International Journal of Solids and Structures* (submitted)	Dec. 2004
1056	Fulton, J. M., S. Hussain, J. H. Lai, M. E. Ly, S. A. McGough, G. M. Miller, R. Oats, L. A. Shipton, P. K. Shreeman, D. S. Widrevitz, and E. A. Zimmermann	Final reports: Mechanics of complex materials, Summer 2004 (K. M. Hill and J. W. Phillips, eds.)	Dec. 2004
1057	Hill, K. M., G. Gioia, and D. R. Amaravadi	Radial segregation patterns in rotating granular mixtures: Waviness selection—*Physical Review Letters*, in press (2004)	Dec. 2004
1058	Riahi, D. N.	Nonlinear oscillatory convection in rotating mushy layers—*Journal of Fluid Mechanics* (submitted)	Dec. 2004
1059	Okhuysen, B. S., and D. N. Riahi	On buoyant convection in binary solidification—*Journal of Fluid Mechanics* (submitted)	Jan. 2005
1060	Brown, E. N., S. R. White, and N. R. Sottos	Retardation and repair of fatigue cracks in a microcapsule toughened epoxy composite—Part I: Manual infiltration—*Composites Science and Technology* (submitted)	Jan. 2005
1061	Brown, E. N., S. R. White, and N. R. Sottos	Retardation and repair of fatigue cracks in a microcapsule toughened epoxy composite—Part II: *In situ* self-healing—*Composites Science and Technology* (submitted)	Jan. 2005